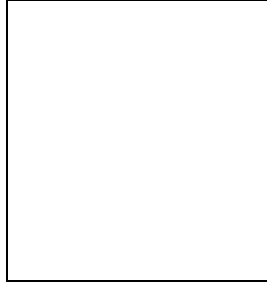


Dark Matter from the Inert Doublet Model

Laura Lopez Honorez

*Service de Physique Théorique, Université Libre de Bruxelles,
CP225, Bld du Triomphe, 1050 Brussels, Belgium*



The Inert Doublet Model is an extension of the Standard Model including one extra “Inert scalar doublet” and an exact Z_2 symmetry. The “Inert scalar” provides a new candidate for dark matter. We present a systematic analysis of the dark matter abundance assuming the standard freeze-out mechanism and investigate the potentialities for direct and gamma indirect detection. We show that the dark matter candidate saturates the WMAP dark matter density in two rather separate mass ranges, one between 40 and 80 GeV, the other one over 400 GeV. We also show that the model should be within the range of future experiments, like GLAST and EDELWEISS II or ZEPLIN.

1 Introduction

Many evidences for the existence in the universe of dark matter has been put forward over the years. It can be inferred from the dynamics of galaxies and of clusters of galaxies, from analysis of the CMBR, from structure formation, etc. The question that arises then is what is the nature of dark matter and which extension of the Standard Model do we have to consider in order to account for these observations? A profusion of models of dark particles have been proposed over the years and it is much hoped that present and forthcoming experiments will throw some light on the matter (for a review, see for instance¹).

In these proceedings, we study a simple extension of the Standard Model with one extra scalar doublet and an exact Z_2 symmetry. In this framework, the candidate for dark matter is one of the two neutral scalars arising from the extra doublet. The latter was called “Inert doublet” by Barbieri *et al* in² because it has no direct coupling to matter fields. However it couples to the standard gauge fields. The phenomenology of its neutral and charged components is quite simple and yet very rich.

This is not the only attractive feature of the model. As was pointed out in², the Inert Doublet Model (IDM) could allow for a Higgs mass up to 500 GeV still fulfilling the LEP Electroweak

Precision Test measurements. Here, we will only consider a Higgs with a mass of 120 GeV. In the reference paper³, one can find a more detailed study of the IDM with Higgs masses of 120 GeV and 200 GeV (See also⁴ where the authors considered Higgs masses up to 500 GeV). Another interesting aspect of models like the IDM is that it could pave the way toward an understanding of the relation between the abundance of dark and ordinary matter (see *e.g.*⁵).

2 Short description of the Model

The IDM is a particular two Higgs doublet model, in which one of the doublet, H_1 , plays the role of the standard Brout-Englert-Higgs doublet while the second one, H_2 , is the source for dark matter candidates. In order to guarantee the stability of the dark matter particles, one invoke a Z_2 symmetry under which all Standard Model fields are even and

$$H_1 \rightarrow H_1 \text{ and } H_2 \rightarrow -H_2.$$

This discrete symmetry also prevents the appearance of flavor changing neutral currents in this model. Moreover, we assume that Z_2 is not spontaneously broken. This model was first introduced by Deshpande and Ma⁶ (see also⁷), and the dark matter aspect was recently discussed by Cirelli *et al*⁸ and Barbieri *et al*². Their initial purpose and some of their assumptions were nevertheless not exactly identical. In addition, the neutral scalar reaching the dark matter WMAP abundance was found to be in the mass range of 60 to 75 GeV for Barbieri *et al*² while for Cirelli *et al*⁸ it was of order of 430 GeV. We first study the details of the model before to elucidate this apparent incompatibility.

The most general potential of the model can be written as

$$V = \mu_1^2 |H_1|^2 + \mu_2^2 |H_2|^2 + \lambda_1 |H_1|^4 + \lambda_2 |H_2|^4 + \lambda_3 |H_1|^2 |H_2|^2 + \lambda_4 |H_1^\dagger H_2|^2 + \frac{\lambda_5}{2} [(H_1^\dagger H_2)^2 + h.c.] \quad (1)$$

The vacuum expectation value of H_1 is given by $\langle H_1 \rangle = \frac{v}{\sqrt{2}}$ with $v = \sqrt{-\mu_1^2/\lambda_1} = 248$ GeV, while assuming for simplicity $\mu_2^2 > 0$, we have $\langle H_2 \rangle = 0$. The mass of the Higgs particle h is $M_h^2 = -2\mu_1^2 \equiv 2\lambda_1 v^2$ while the mass of the charged, H^\pm , and two neutral, H_0 and A_0 , components of the field H_2 are given by

$$\begin{aligned} M_{H^\pm}^2 &= \mu_2^2 + \lambda_3 v^2/2 \\ M_{H_0}^2 &= \mu_2^2 + (\lambda_3 + \lambda_4 + \lambda_5)v^2/2 \\ M_{A_0}^2 &= \mu_2^2 + (\lambda_3 + \lambda_4 - \lambda_5)v^2/2. \end{aligned} \quad (2)$$

For appropriate quartic couplings, H_0 or A_0 is the lightest component of the H_2 doublet. In the absence of any other lighter Z_2 -odd field, either one is a candidate for dark matter. For definiteness we choose H_0 . All our conclusions are unchanged if the dark matter candidate is A_0 instead. Following², we parameterize the contribution from symmetry breaking to the mass of H_0 by $\lambda_L = (\lambda_3 + \lambda_4 + \lambda_5)/2$, which is also the coupling constant between the Higgs field h and our dark matter candidate H_0 .

3 Dark matter abundance

As in² and in⁸, we consider a thermal production of the cold relic H_0 . We have computed the relic abundance of H_0 using micrOMEGAs2.0, a new and versatile package for the numerical calculation of dark matter abundance from thermal freeze-out⁹.

We first present the results for fixed Inert scalars mass differences in the contour plots of figure 1. We work in the (M_{H_0}, μ_2) plane, as a result the diagonal line corresponds to $\lambda_L = 0$, *i.e.* to no coupling between H_0 and the Higgs boson. Away from this line, λ_L increases, with

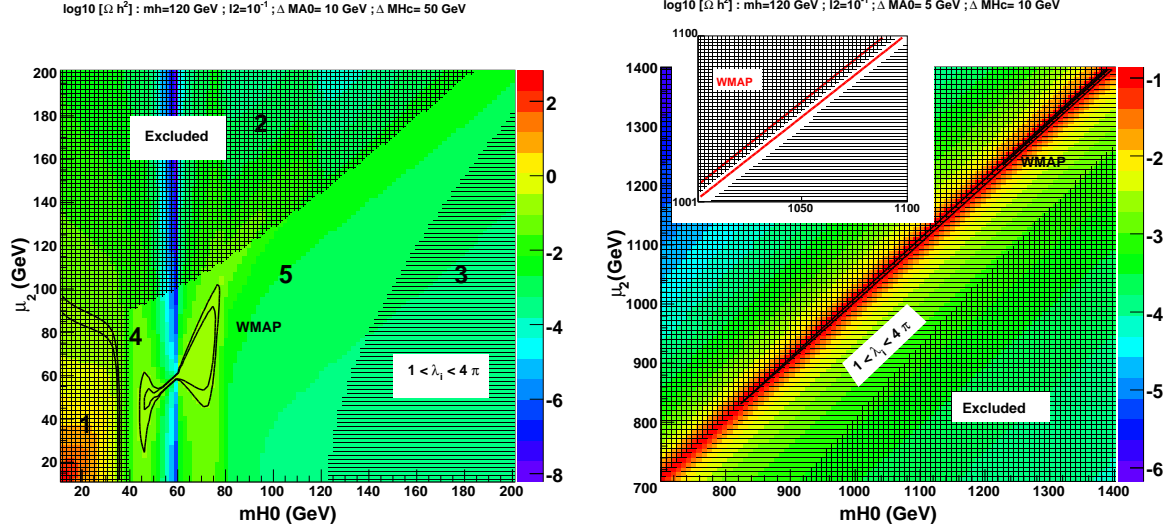


Figure 1: Relic density contours in the (M_{H_0}, μ_2) plane for $M_h = 120$. Left: low mass regime with Inert scalars mass differences $\Delta M_{A_0} = 10$ GeV and $\Delta M_{H^+} = 50$ GeV. Right: high mass regime with Inert scalars mass differences $\Delta M_{A_0} = 5$ GeV and $\Delta M_{H^+} = 10$ GeV.

$\lambda_L < 0$ (resp. $\lambda_L > 0$) above (resp. below) the diagonal. Also, we write $\Delta M_{A_0} = M_{A_0} - M_{H_0}$ and $\Delta M_{H_c} = M_{H^+} - M_{H_0}$.

The shaded areas in the plots correspond to regions that are excluded by several constraints. In order not to conflict with LEP data, the mass of the H^+ should be larger than 79.3 GeV and $M_{H^0} + M_{A^0} \lesssim M_Z$. These constraints translate into the excluded region 1 on the plot on the left of figure 1. The vacuum stability constraint contributes largely to the exclusion of $\lambda_L < 0$ couplings. This corresponds to shaded area in the domains $\mu_2 > M_{H_0}$ in the plots of figure 1. The remaining shaded regions are excluded due to large couplings $|\lambda_i| > 4\pi$. Moreover regions where the couplings range as $1 < |\lambda_i| < 4\pi$, which is still tolerable, are shown with horizontal lines. The areas between two dark lines correspond to regions of the parameter space such that $0.094 < \Omega_{DM} h^2 < 0.129$, the range of dark matter energy densities consistent with WMAP data.

We immediately see that there are two qualitatively distinct regimes, depending on whether the H_0 is lighter than the W and Z and/or the Higgs boson. For the low mass regime, let us study figure 1, the plot on the left. The two processes relevant below the W , Z or h threshold are the H_0 annihilation through the Higgs and H_0 coannihilation with A_0 through Z exchange^a. Both give fermion-antifermion pairs, the former predominantly into $b\bar{b}$. Coannihilation into a Z may occur provided ΔM_{A_0} is not too important, roughly ΔM_{A_0} must be of order of $T_{fo} \sim M_{H_0}/25$. As the mass of H_0 goes above W , Z or h threshold, H_0 annihilation into WW , ZZ and hh become increasingly efficient, an effect which strongly suppresses the H_0 relic density. The region 4 of figure 1, corresponding to $M_{H_0} \in [40, 80]$ GeV, appears to be the only region consistent with WMAP data.

For the high mass regime, we can derive the general trends from figure 1, the plot on the right. No new annihilation channel opens if M_{H_0} is heavier than the Higgs or the gauge bosons. There are then essentially two kinds of processes which control both the abundance: the annihilation into two gauge bosons, dominant if $\mu_2 < M_{H_0}$, and the annihilation into two Higgs, which dominates if $\mu_2 > M_{H_0}$. Coannihilation plays little role.

The abundance of dark matter is suppressed over most of the area of the plot because of large quartic coupling effects on the cross-sections. Let us emphasize that in this regime, it is

^a $H_0 H^+$ coannihilation is suppressed for our choice of ΔM_{H_c} .

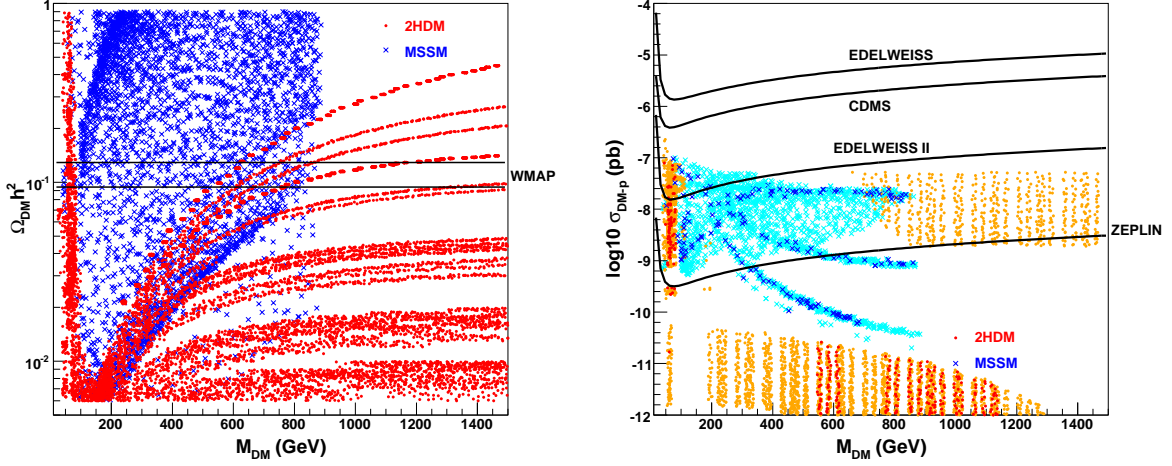


Figure 2: Left: Relic density and Right: scattering cross-section intervening in direct detection searches, all as a function of the mass of dark matter and comparison with the MSSM. For the direct detection plot, the light colors correspond to $0.01 < \Omega_{DM} h^2 < 0.3$, while the dark colors correspond to $0.094 < \Omega_{DM} h^2 < 0.129$.

possible to reach agreement with WMAP data, but only at the price of some fine tuning. We need to keep the mass splittings between the components of H_2 relatively small. First because large mass splittings correspond to large couplings and second because the different contributions to the annihilation cross-section must be suppressed at the same location, around $\lambda_L = 0$ (*i.e.* $M_{H_0} \simeq \mu \simeq M_{A_0} \simeq M_{H_+}$ in this case). As it can be seen in figure 1, the plot on the right, the area consistent with WMAP corresponds to the narrow region around the diagonal with $M_{H_0} \gtrsim 800$ GeV for $\Delta M_{A_0} = 5$ GeV and $\Delta M_{H_c} = 10$ GeV. Notice that this behavior is limited by the unitarity bound on the total annihilation cross-section¹⁰ which constrains the mass of the dark particle to be $M_{H_0} \lesssim 120$ TeV.

In figure 2, the plot on the left, we show a scatter plot of $\Omega_{DM} h^2$ as a function of the mass of the dark matter candidate M_{DM} for a fair sample of IDMs (scanning on several Inert scalar mass splittings) and, for the sake of comparison, for the MSSM. We clearly see the two regimes (low mass and high mass) of the IDM that may give rise to a relevant relic density (*i.e.* near WMAP). The MSSM models have a more continuous behavior, with $\mathcal{O}(100$ GeV) dark matter masses. As a conclusion, the IDM provides dark matter candidates with masses as small as 40 GeV and as large as 600 GeV in contrast with the MSSM more concentrated around ~ 100 GeV.

4 Direct detection

Direct detection searches look for signals of dark matter in low background detectors trying to measure the energy deposited by the scattering of a dark matter particle with a nucleus of the detector. Assuming that the main interaction contributing to the H_0 -quarks interaction is the spin independent $H_0 q \xrightarrow{h} H_0 q$ interaction^b it can be shown² that the H_0 elastic scattering cross section off a proton scales like

$$\sigma_{H_0-p} \propto \lambda_L^2 / (M_{H_0} M_h^2)^2. \quad (3)$$

In figure 2, the plot on the right, we show a scatter plot of $\log_{10} \sigma_{DM-p}$ as a function of M_{DM}

^bThe experiments have reached such a level of sensitivity that the Z exchange contribution $H_0 q \xrightarrow{Z} A_0 q$ is excluded by the current experimental limits². Consequently, to forbid Z exchange by kinematics, the mass of the A_0 particle must be larger than the mass of H_0 by a few 100 keV.

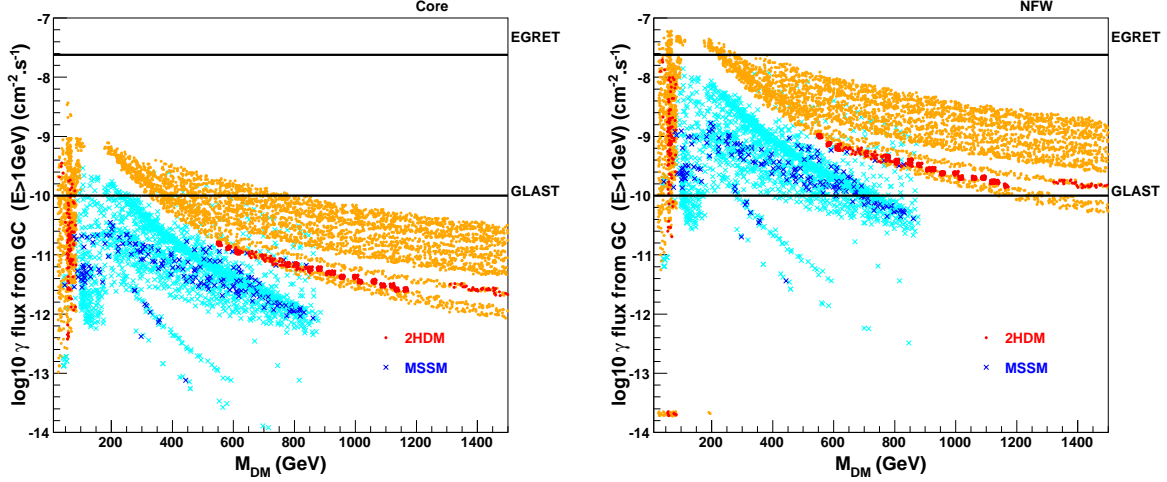


Figure 3: Integrated gamma-ray flux from the Galactic Center (GC) resulting from dark matter annihilation as a function of the mass of the dark matter candidate for the same sample of models than for direct detection in Fig.2. Again, the light colors correspond to $0.01 < \Omega_{DM} h^2 < 0.3$, while the dark colors correspond to $0.094 < \Omega_{DM} h^2 < 0.129$. For the plot on the left, we took an isothermal profile (flat profile), for the plot on the right, we took a NFW profile (more steeper at Galactic Center).

for the IDMs considered in the abundance plot of figure 2 that account for $0.01 < \Omega_{DM} h^2 < 0.3$. We see that the low mass regime candidates could be detected by future experiments such as EDELWEISS II or by the ton sized experiments such as ZEPLIN. For the higher mass regime however, there is no hope for future detection in low background detector. Indeed, the WMAP requirement for dark matter relic density constrains the λ_L couplings to be vanishing while the same couplings drive the amplitude of the matter- H_0 scattering cross-section.

5 Indirect detection

The measurement of secondary particles coming from dark matter annihilation in the halo of the Galaxy is another promising way of deciphering the nature of dark matter. Let us emphasize that this possibility depends however not only on the properties of the dark matter particle, through its annihilation cross-sections, but also on the astrophysical assumptions made concerning the distribution of dark matter in the halo that supposedly surrounds our Galaxy.

In Figure 3, we show the log of the produced gamma-ray flux from dark matter annihilation at the Galactic Center Φ_γ as a function of M_{DM} for the same sample of models than for direct detection. We computed the gamma-ray flux for the plot on the left assuming an isothermal dark matter density profile while for the plot on the right we assumed a Navarro, Frank and White (NFW) profile. The main difference between these two profiles is the slope of the dark matter density as a function of the galactic radius in the central part of the Galaxy. The isothermal profile is flat while the NFW profile is more cuspy (*i.e.* steeper). We see that for steeper profile the gamma-ray flux is larger.

The particle physics dependence of Φ_γ also clearly show up in figure 3. Indeed we see that Φ_γ behaves differently in the low and the high mass regime of the IDM given that the processes contributing to the annihilation cross-section are different. Moreover, notice that the IDM dark matter candidates have typically higher detection rates than the neutralino in SUSY models, especially at high mass. Let us stress that the figures for indirect detection were obtained taking into account annihilation processes at three level only (see ⁴, for a recent study of the IDM

including processes at one-loop). It can be inferred from figure 3 that the IDM can give the right relic abundance in a range of parameters which will be probed by GLAST for NFW dark matter profiles. GLAST will however have no chance to observe the gamma-ray flux produced by annihilating H_0 at the Galactic Center for flatter profiles such as the isothermal one.

6 Conclusion

We carried out a rather detailed analysis of the IDM as a dark matter model assuming the standard freeze-out mechanism. We recovered the results of Barbieri *et al.* and Cirelli *et al.* which a priori did not seem to match. This is because the IDM provides dark matter candidates in two rather separate mass ranges, one between 40 and 80 GeV, the other one over 400 GeV. The physics driving the existence of dark matter in these regions of the parameter space is quite different.

We have also investigated the prospects for direct and indirect detection searches. Concerning direct detection searches, the low mass regime candidates should be detected with the futures ton sized experiments while the high mass regime will stay out of reach. For indirect detection searches we looked at the gamma-ray flux generated at the Galactic Center by dark matter annihilation. Whatever the dark matter density profile assumed, we have come to the conclusion that the Inert scalars have typically higher detection rates than the neutralino in SUSY models, especially at high mass. Moreover, the IDM could be probed by the future GLAST experiment.

Acknowledgments

This work is supported by the FNRS, the I.I.S.N. and the Belgian Federal Science Policy (IAP 5/27).

References

1. Gianfranco Bertone, Dan Hooper, and Joseph Silk. Particle dark matter: Evidence, candidates and constraints. *Phys. Rept.*, 405:279–390, 2005.
2. Riccardo Barbieri, Lawrence J. Hall, and Vyacheslav S. Rychkov. Improved naturalness with a heavy higgs: An alternative road to lhc physics. *Phys. Rev.*, D74:015007, 2006.
3. Laura Lopez Honorez, Emmanuel Nezri, Josep L. Oliver, and Michel H. G. Tytgat. The inert doublet model: An archetype for dark matter. *JCAP*, 0702:028, 2007.
4. Michael Gustafsson, Erik Lundstrom, Lars Bergstrom, and Joakim Edsjo. Significant gamma lines from inert higgs dark matter. 2007.
5. Pei-Hong Gu, Hong-Jian He, and Utpal Sarkar. Dirac neutrinos, dark energy and baryon asymmetry. 2007.
6. Nilendra G. Deshpande and Ernest Ma. Pattern of symmetry breaking with two higgs doublets. *Phys. Rev. D*, 18(7):2574–2576, Oct 1978.
7. Ernest Ma. Verifiable radiative seesaw mechanism of neutrino mass and dark matter. *Phys. Rev.*, D73:077301, 2006.
8. Marco Cirelli, Nicolao Fornengo, and Alessandro Strumia. Minimal dark matter. *Nucl. Phys.*, B753:178–194, 2006.
9. G. Belanger, F. Boudjema, A. Pukhov, and A. Semenov. micromegas2.0: A program to calculate the relic density of dark matter in a generic model. 2006.
10. Kim Griest and Marc Kamionkowski. Unitarity limits on the mass and radius of dark matter particles. *Phys. Rev. Lett.*, 64:615, 1990.